FOCUSED TOPIC

Virulence Evolution of Pathogens That Can Grow in Reservoir Environments*

Aakash Pandey,[1],[†] **Nicole Mideo,**[2] **and Thomas G. Platt**[1]

1. Division of Biology, Kansas State University, Manhattan, Kansas 66506;   2. Department of Ecology and Evolutionary Biology, University of Toronto, Toronto, Ontario, Canada

ABSTRACT: Many pathogens reside in environmental reservoirs within which they can reproduce and from which they can infect hosts. These facultative pathogens experience different selective pressures in host-associated environments and reservoir environments. Heterogeneous selective pressures have the potential to influence the virulence evolution of these pathogens. Previous research has examined how environmental transmission influences the selective pressures shaping the virulence of pathogens that cannot reproduce in environmental reservoirs, yet many pathogens of humans, crop plants, and livestock can reproduce in these environments. We build on this work to examine how reproduction in reservoirs influences disease dynamics and virulence evolution in a simple facultative pathogen model. We use adaptive dynamics to examine the evolutionary dynamics of facultative pathogens under potential trade-offs between transmission and virulence, shedding and virulence, and reservoir persistence and virulence. We then perform critical function analysis to generalize the results independent of specific trade-off assumptions. We determine that diverse virulence strategies, sometimes resulting from evolutionary bistability or evolutionary branching conditions, are expected for facultative pathogens. Our findings motivate research establishing which trade-offs most strongly influence the virulence evolution of facultative pathogens.

Keywords: adaptive dynamics, life history trade-off, heterogeneous selection, opportunistic infection, environmental transmission.

Introduction

Life history trade-offs reflect constraints that ensure that changes in one trait result in fitness costs associated with another trait (Charnov 1989; Stearns 1989; Roff 2000). Pathogens can experience trade-offs associated with various traits

that influence their fitness. Many pathogens reproduce within hosts and in environmental reservoirs and consequently experience heterogeneous selective pressures. These facultative pathogens include environmental opportunists like *Vibrio cholerae* and *Bacillus anthracis*, the etiological agents of cholera and anthrax, and commensal opportunists like *Candida albicans* and *Streptococcus pneumoniae*, the etiological agents of candidiasis and pneumococcal diseases (Brown et al. 2012). Most theoretical studies of virulence evolution focus on trade-offs experienced by obligate pathogens (Anderson and May 1978; Ewald 1983; van Baalen and Sabelis 1995; Frank 1996; Alizon et al. 2009; Cressler et al. 2016). The heterogeneous selective pressures faced by pathogens that can infect from environmental reservoir populations are thought to relax the virulence-transmission trade-off, resulting in higher overall virulence (Ewald 1983, 1991*a*, 1991*b*; Bonhoeffer et al. 1996; Gandon 1998; Day 2002*a*; Walther and Ewald 2004; Roche et al. 2011; Boldin and Kisdi 2012). Selection in environments where pathogens do not cause disease can influence the virulence evolution of opportunistic pathogens when there are correlations between the pathogen's population dynamics in these environments and in environments where they do cause disease (Brown et al. 2012). However, no theoretical study of virulence evolution has allowed for pathogen replication in the environmental reservoir, although some studies have examined the epidemiological dynamics of facultative pathogens (Godfray et al. 1999; Bani-Yaghoub et al. 2012; Kaitala et al. 2017; Lanzas et al. 2019).

The environment in which facultative pathogens live and reproduce varies over space and time—with host and reservoir environments imposing different requirements for survival and reproduction. Consequently, these organisms routinely experience heterogeneous selective pressures (Caraco and Wang 2008; Mikonranta et al. 2012, 2015; Barton et al.

2018). The importance of heterogeneous selection pressures on virulence evolution has already been highlighted in the context of multihost pathogen systems (Regoes et al. 2000; Gandon 2004). Owing to their life history, with a population stage structured in host and reservoir environments, novel trait correlations and trade-offs can impact the course of virulence evolution in these pathogens (Sokurenko et al. 2006; Brown et al. 2012; Barton et al. 2018). For example, traits influencing the environmental persistence of free-living pathogens can be correlated with virulence, potentially resulting in a trade-off between these functions. Consistent with a relationship between virulence and antipredation traits that promote environmental persistence, the experimental evolution of the opportunistic pathogen *Serratia marcescens* in the presence of a protozoan predator results in reduced virulence (Friman et al. 2009; Mikonranta et al. 2012). Similarly, the evolution of the facultative fish pathogen *Flavobacterium columnarae* in the presence of lytic phages similarly reduces virulence (Laanto et al. 2012). Because of associations between virulence and traits that affect functions in reservoir environments, selection in these environments likely influences the degree of virulence facultative pathogens exhibit.

The importance of reservoir dynamics to the evolution of virulence may depend on the context-dependent fitness consequences of virulence factors. Costs stemming from the expression of virulence factors or the maintenance of genes encoding virulence factors (Sturm et al. 2011; Platt et al. 2012; Peyraud et al. 2016; Pilla et al. 2017) may adversely affect the fitness of facultative pathogens in reservoir environments—where the benefits of pathogenesis are absent. For this reason, costs associated with virulence factors may result in a negative correlation between virulence and environmental persistence—a relationship that may influence the virulence evolution of facultative pathogens. The virulence factors of some facultative pathogens may alternatively have a function promoting the persistence of the pathogen in the environmental reservoir. For example, Shiga toxin, produced by *Escherichia coli* and *Shigella* sp. pathogens, may function in promoting both virulence and resistance to grazing by protozoan predators (Steinberg and Levin 2007; Adiba et al. 2010). Similarly, virulence factors may mediate interspecific competition in the reservoir environments in addition to mediating the virulence of facultative pathogens (Anttila et al. 2013). For example, in the facultative pathogen *Stenotrophomonas maltophilia*, a type 4 secretion system is involved in competition against heterologous bacteria and is also responsible for apoptosis of human macrophages such that a shared mechanism links virulence and competitive ability (Bayer-Santos et al. 2019; Nas et al. 2019). The dual function of these virulence factors, reflecting either preadaptation or coincidental selection of traits impacting virulence (Levin 1996; Brown et al. 2012), may result in a positive correlation between virulence and environmental persistence of these facultative pathogens.

One main challenge for studying the virulence evolution in facultative pathogens is adequately defining pathogen fitness, since infecting a new host is no longer the only way for a pathogen to reproduce. Although the basic reproduction number is used as a fitness proxy in most theoretical studies of virulence evolution, it is not a suitable fitness proxy in many epidemiological settings (Lion and Metz 2018). In the case of facultative pathogens, the basic reproduction number is an inadequate fitness metric because it omits the consequences of reservoir dynamics. In this study, we consider a simple epidemiological model of a facultative pathogen where we highlight the challenges associated with deriving and interpreting the basic reproduction number. We then derive the invasion fitness for the system of facultative pathogens using the adaptive dynamics framework to examine the evolutionary outcomes for virulence, influenced by potential trade-offs between that trait and transmission, shedding, or persistence. We begin by considering individual trade-offs and later explore evolutionary outcomes when there are multiple trade-offs. We then perform critical function analysis, which allows us to identify evolutionary outcomes independent of specific trade-off assumptions. Evolution under individual trade-offs can result in intermediate or high virulence if the fitness gain from increasing the correlated trait (transmission, shedding, or persistence) more than compensates the fitness loss due to increased virulence. Otherwise, low virulence or avirulence is expected. More diverse evolutionary outcomes are predicted when we consider multiple, simultaneous trade-offs influencing virulence evolution. We observed bistability conditions under a wide range of parameters. Similarly, evolutionary branching points occur in multiple scenarios, suggesting that diverse virulence strategies are possible in facultative pathogens. Hence, our work lays the foundation for a more system-specific exploration of virulence evolution in facultative pathogens.

Model

We extended the modeling approach described by Boldin and Kisdi (2012) to capture a system in which a pathogen can be transmitted both directly from hosts and indirectly through the environment by allowing the pathogen to reproduce in the environment. In so doing, our model describes the population dynamics of facultative pathogens such as *Vibrio cholerae*, *Bacillus anthracis*, and *Stenotrophomonas maltophilia*. This model describes a system composed of susceptible hosts (S), infected hosts (I), and a pathogen reservoir (P). The pathogen is present in both infected hosts and an environmental reservoir where it reproduces. Susceptible hosts can become infected following contact with either infected

hosts or the environmental reservoir. The relative contribution of each transmission route to the disease dynamics likely differs across disease systems. In some cases both transmission routes can be significant (e.g., cholera; Tien et al. 2011), whereas in many other waterborne pathogens environmental transmission is likely more important than direct transmission (Julian 2016). Hence, we include both transmission routes to keep the model general. The flow diagram in figure 1 illustrates the relationships among the *S*, *I*, and *P* compartments.

The following system of ordinary differential equations describes the system illustrated by figure 1:

$$\frac{dS}{dt} = b - \beta SI - \gamma S \frac{\phi P}{P + \tau} - dS,$$

$$\frac{dI}{dt} = \beta SI + \gamma S \frac{\phi P}{P + \tau} - (d + \rho + \alpha)I, \qquad (1)$$

$$\frac{dP}{dt} = \theta I - \sigma P + rP\left(1 - \frac{P}{K}\right).$$

We assume that susceptible hosts are born at a constant rate (*b*) and die at a per capita rate (*d*), with direct infection following mass action incidence with rate constant β. The recovery rate is given by ρ, and we assume lifelong immunity once the host is recovered. Although we assume ρ to be zero in simulation results, we have not dropped it from analytic expressions to make them applicable to broader scenarios. We assume that the contact rate between susceptible hosts and pathogens in the environmental reservoir is an increasing but saturating function of *P*, described by $\phi P/(P + \tau)$. Although there is little empirical data for any system with which to define an exact analytical form for environmental transmission, this form of environmental transmission is used by several studies because it incorporates concentration-dependent pathogen transmission from the environment (Codeço 2001) and
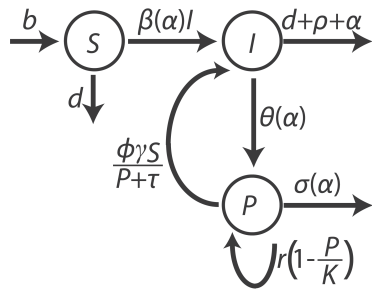
is analytically tractable (Roche et al. 2011; Boldin and Kisdi 2012; Breban 2013). For simplicity, we assume $\phi = 1$ and $\tau = 1$. The term γ represents the probability of environmental transmission on contact with pathogens in the reservoir. The loss of free-living pathogens from the reservoir due to the uptake by host is assumed to be negligible. Free-living pathogen population dynamics depend on shedding from infected hosts at rate θ, death of free-living pathogen propagules at rate σ, and density-dependent (specifically, logistic) reproduction of pathogen propagules at per capita rate *r*.

Trade-offs are represented by functional relationships between traits. As in Boldin and Kisdi (2012), we consider the trade-off between (direct) transmission and virulence where transmission is a saturating function of virulence, $\beta(\alpha) = c\alpha/(c\alpha + h)$. While several studies have documented such a trade-off, a recent meta-analysis identified that there have been insufficient empirical studies evaluating trade-offs between virulence and transmission (Acevedo et al. 2019). Furthermore, we know of no studies directly evaluating this relationship for a facultative pathogen. If virulence is directly correlated with the pathogen population size within a host, then the degree of pathogen shedding by an infected host may depend on virulence. For example, virulence and duration of infection is shown to be correlated with within-host pathogen number in the facultative pathogen *S. maltophilia* (White et al. 2016). High-virulence strains cause greater intestinal distension and are potentially shed from hosts at a higher rate, either continuously during infection or abruptly following death of the host. We consider the case of continuous shedding in our model. As in direct transmission-virulence trade-off, we consider a case where the shedding rate increases monotonically with virulence. Specifically, we assume the following functional relationship between shedding and virulence: $\theta(\alpha) = g\alpha/(g\alpha + f)$.

We also consider two potential relationships between reservoir persistence (i.e., the inverse of pathogen death rate in the reservoir) and virulence. First, strategies that enhance a facultative pathogen's survival in the reservoir can also result in higher virulence within a host as a result of preadaptation or coincidental evolution. For example, antipredator adaptations in the reservoir environment could function as virulence factors within a host (Adiba et al. 2010; Robino et al. 2019). As a result, pathogen persistence and virulence may trade off, since increased persistence positively impacts pathogen fitness whereas virulence results in a fitness cost due to death of the host, reducing the infectious period. We assume that the pathogen death rate in the reservoir decreases (equivalently, persistence increases) as a function of virulence and is given as $\sigma(\alpha) = e^{-u\alpha} + v$. Under this relationship, the free-living propagules of a strain that does not harm the host ($\alpha = 0$) are expected to survive in the environmental reservoir for $1/(1 + v)$ units of time, whereas

Figure 1: Schematic representation of the model described by system (1). *S* and *I* represent the number of susceptible and infected hosts, respectively. *P* represents the number of free-living propagules in an environmental reservoir. See table 1 for variable and parameter definitions.

Table 1: Definitions of the symbols used in the model

Symbol	Definition	Value (dimension)
S	Number of susceptible hosts	... (N)
I	Number of infected hosts	... (N)
P	Number of free pathogens	... (N)
b	Birth rate of hosts	1 (N time^{-1})
d	Per capita death rate of hosts	.2 ($N\,N^{-1}$ time^{-1})
α	Per capita disease induced death rate (virulence) of hosts	Varies ($N\,N^{-1}$ time^{-1})
ρ	Per capita recovery rate of hosts	0 ($N\,N^{-1}$ time^{-1})
θ	Per host shedding rate	Varies ($N\,N^{-1}$ time^{-1})
β	Transmission rate	Varies (N^{-1} time^{-1})
γ	Probability of infection on contact between susceptible-free pathogen	.35 (...)
r	Per capita birth rate of environmental propagules	.1 ($N\,N^{-1}$ time^{-1})
K	Carrying capacity of population of pathogen propagules in the reservoir	Varies (N)
σ	Free pathogen death rate	Varies ($N\,N^{-1}$ time^{-1})

Note: N represents number. For variables and parameters that vary, see individual figure legends for values used.

this time period approaches $1/\nu$ units of time as virulence increases. Caraco and Wang (2008) consider a similar functional relationship where the free-living pathogen persistence increases with increasing virulence. Second, we consider a different functional relationship where increasing virulence is associated with a higher free-living pathogen death rate. This negative correlation between virulence and pathogen persistence in the reservoir environment can occur as a result of energetic constraints, where the pathogen's investment in one environment comes at the cost of reduced performance in another. Specifically, we assume $\sigma(\alpha) = a/(e^{-u\alpha} + \nu)$. In all cases, a, c, f, g, h, u, ϕ, τ, and ν are constants and are positive. Although our simulation results depend on the functional relationships considered, qualitative interpretation of our analytical results are not restricted to specific functional forms.

Evolutionary outcomes in the adaptive dynamics framework are critically dependent on the assumed trade-off shapes. Hence, to identify general results for trade-offs of arbitrary shapes, we follow Kisdi (2006) to perform critical function analysis. The critical function is derived from the invasion fitness, $W(\alpha, \alpha_m)$. Singular strategies occur when the trait correlation is locally tangent to a solution of the critical function. The nature of a singular strategy is determined by evaluating the following second derivatives:

$$E = \left. \frac{\partial^2}{\partial \alpha_m^2} W(\alpha, \alpha_m) \right|_{\alpha_m = \alpha = \alpha^*},$$

$$M = \left. \frac{\partial^2}{\partial \alpha \partial \alpha_m} W(\alpha, \alpha_m) \right|_{\alpha_m = \alpha = \alpha^*}.$$

Here, α_m represents the mutant trait value, whereas α^* is the singular trait. The singular trait is convergence stable if $E + M < 0$ and is evolutionarily stable if $E < 0$. Evolu-

tionary branching points occur when the singular strategy is convergence stable but not evolutionarily stable.

Results

Epidemiological Results

System (1) has a disease-free equilibrium (DFE) point (S_0, I_0, P_0) given by $(b/d, 0, 0)$. The stability of this equilibrium is determined by the eigenvalue of the Jacobian evaluated at this DFE. If the eigenvalue is greater than zero, the DFE is unstable, whereas if the eigenvalue is less than zero, the DFE is stable (appendix, sec. A1; the appendix is available online). Alternatively, the Jacobian can be reframed into a next-generation matrix whose spectral radius (λ) determines the stability of the DFE (Diekmann et al. 2009). We focused on this threshold parameter of the next-generation matrix in our description of the stability of DFE because it is easier to interpret and can be related to another important epidemiological threshold parameter, the basic reproduction number (R_0). The spectral radius (λ) of the next-generation matrix (eq. [A1.4]) for system (1) evaluated at the DFE is

$$\lambda = \frac{1}{2} \left(\frac{\beta S_0}{(d + \rho + \alpha)} + \frac{r}{\sigma} \right.$$
$$\left. + \sqrt{\left(\frac{\beta S_0}{(d + \rho + \alpha)} - \frac{r}{\sigma} \right)^2 + 4 \frac{\gamma S_0}{\sigma} \frac{\theta}{(d + \rho + \alpha)}} \right).$$
$$(2)$$

The DFE is stable if $\lambda \leq 1$ and is unstable if $\lambda > 1$. The DFE can be stable only if the free-living pathogen death rate, σ, is greater than its birth rate, r, in the environmental reservoir (appendix, sec. A1). Assuming that the pathogen cannot reproduce in the reservoir (i.e., $r = 0$) and that there is no

environmental infection (i.e., $\gamma = 0$), then equation (2) reduces to $\lambda = \beta S_0 / (d + \rho + \alpha)$, which is also the expression of R_0 for a simple model of a directly transmitted obligate pathogen (e.g., Anderson and May 1981).

Although λ is a threshold parameter, we refrain from calling it the basic reproduction number. In the derivation of λ, we include the birth of facultative pathogens in the reservoir together with the epidemiological "births" in the "transmission" matrix (appendix, sec. A1). Thus, λ is not equal to the expected number of infections caused by a single infected individual in an otherwise susceptible population (i.e., R_0). Instead, λ is the demographic reproduction number representing per-generation overall growth of the facultative pathogen, which is distinct from R_0, the epidemiological basic reproduction number (for a review of R_0 and its relation to demography, see Heesterbeek 2002).These parameters, λ and R_0, are interchangeable when the transmission matrix includes only one type of birth (i.e., the epidemiological birth), as is the case in Boldin and Kisdi (2012; but see the appendix, sec. A2). In contrast, λ and R_0 are qualitatively and quantitatively different for models where the pathogen can reproduce independent of focal host (e.g., facultative pathogens).

If the birth of different "types" have nonzero entries in the transmission matrix, then R_0 for such a system can be de-

fined as a form of type reproduction number (Roberts and Heesterbeek 2003; Heesterbeek and Roberts 2007; van den Driessche 2017). Following the procedure of deriving the type reproduction number, a general expression for R_0 can be derived as

$$R_0 = R_{0d} + \frac{\gamma S_0}{\sigma} \frac{\theta}{d + \rho + \alpha} \left(\frac{r}{\sigma} + \left(\frac{r}{\sigma} \right)^2 + \cdots \right), \quad (3)$$

where

$$R_{0d} = \frac{\beta S_0}{d + \rho + \alpha} + \frac{\gamma S_0}{\sigma} \frac{\theta}{d + \rho + \alpha}. \quad (4)$$

The term R_{0d} represents the expected number of new infections resulting directly from a single infected individual and the propagules it sheds before they reproduce in the reservoir. The remaining terms on the right-hand side of equation (3) represent the expected number of infections due to the growth of the shed pathogens in the reservoir. Hence, this partitioning of the basic reproduction number is helpful in highlighting the importance of growth in the reservoir to disease dynamics (fig. 2a). In figure 2a, R_{0d} is less than 1 over a considerable parameter space (gray region), but the disease still spreads, as reflected by λ and R_0 both exceeding 1. Here, the disease is endemic because
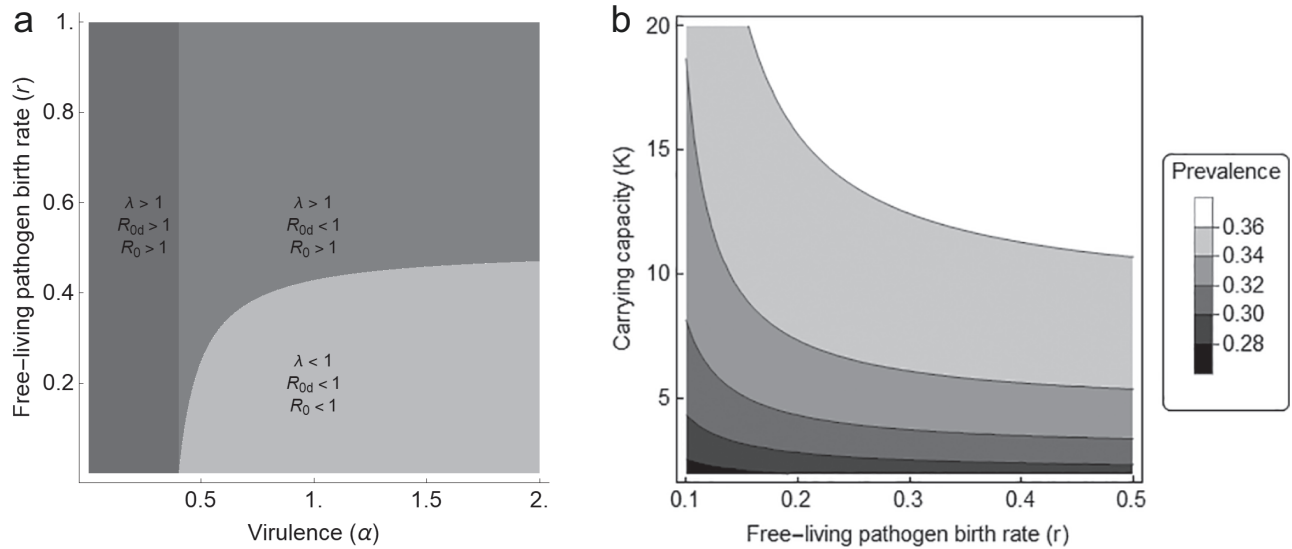

Figure 2: Epidemiological predictions of the facultative pathogen model. *a*, Spectral radius λ (eq. [2]), R_0 (eq. [3]), and R_{0d} (eq. [4]) contour plots showing different epidemiological outcomes. The light gray region corresponds to parameter values where the disease fails to spread at the population level. In the gray region, the spread of the disease requires sufficient reproduction in the environmental reservoir. In the dark gray region, the disease spreads irrespective of the growth rate of the pathogen in the reservoir. Parameter values: $\gamma = 0.1$, $\beta = 0.1$, $\theta = 0.1$, $\sigma = 0.5$. *b*, Effect of pathogen birth rate in the reservoir and environmental carrying capacity on disease prevalence. Increasing birth rate shows little change in endemic disease prevalence, whereas increasing reservoir carrying capacity more strongly impacts prevalence. Parameter values: $\gamma = 0.3$, $\beta = 0.01$, $\theta = 0.1$, $\sigma = 0.1$, $\tau = 1$, $\alpha = 0.3$.

of the frequent introduction of new cases through environmental infection that is dependent on the growth of free-living pathogens. In the dark gray region, the disease spreads irrespective of the growth of pathogen in the reservoir because low virulence allows for a relatively long duration of infection. In the light gray region, disease fails to spread in the population because there is insufficient host-host direct transmission (due to a short duration of infection) coupled with insufficient growth of the pathogen in the reservoir. If $r < \sigma$, the limit of equation (3) exists and can be written as

$$R_0 = \frac{\beta S_0}{d + \rho + \alpha} + \frac{\gamma S_0}{\sigma} \frac{\theta}{d + \rho + \alpha} \left(\frac{1}{1 - (r/\sigma)} \right). \quad (5)$$

However, if $r > \sigma$—that is, the rate at which pathogens reproduce in the environmental reservoir is greater than the rate at which they die—then $R_0 = \infty$ (for a derivation, see the appendix, sec. A2). This is because pathogens shed from a single infected host can cause an unending chain of indirect environmental transmissions from the reservoir population that the pathogen sustains independent of hosts. Although both λ (eq. [2]) and R_0 (eq. [3]) are accurate threshold parameters reflecting disease dynamics (fig. 2a), R_0 is less informative when $r > \sigma$. When the net growth rate of free-living pathogens is positive, we must consider an infinite number of generations of growth for the free-living pathogens shed from a single infected host and the total environmental transmissions resulting from those generations to compute R_0. In practice, we are primarily interested in epidemiological dynamics occurring at short timescales or finite generations. Thus, other metrics, such as epidemic growth rate and disease prevalence (fig. 2b), might be more relevant than R_0.

The reservoir population of facultative pathogens can also influence disease prevalence in the host population. Under the assumption that environmental transmission saturates when the reservoir population is sufficiently dense, we found that the pathogen's birth rate in the reservoir has little effect on the endemic disease prevalence (fig. 2b). The carrying capacity of the reservoir, however, can show significant differences in the level of endemic disease prevalence (fig. 2b).

In our analysis, we have assumed that the disease dynamics start with a single infected host and no pathogens in the environmental reservoir. This may not always be the case. There is another possible DFE that results when $\sigma < r$ and hosts do not contact the pathogen's reservoir population. In this case, the DFE is given as

$$(S_0, I_0, P_0) = \left(\frac{b}{d}, 0, K\left(1 - \frac{\sigma}{r}\right) \right).$$

If the pathogen reservoir and susceptible host population are spatially structured with little or no interaction between the two populations, then S_0 is determined by the host ecology alone and P_0 is determined by the pathogen reservoir ecology alone. When hosts subsequently contact the environmental reservoir, the stability of this DFE is determined by the eigenvalue at this point (appendix, sec. A6).

Epidemiological R_0 Does Not Describe Pathogen Fitness in Facultative Pathogens

In the previous section, we described the limitations of epidemiological R_0 for describing disease dynamics. Historically, the epidemiological R_0 is also considered to be a suitable fitness proxy for evolutionary analysis. However, since R_0 only describes the dynamics of the infected hosts, it largely omits free-living pathogen dynamics. Thus, this epidemiological R_0 often cannot be used as a fitness proxy in evolutionary analysis for facultative pathogens. For example, consider the extreme case where there is little environmental and direct transmission (γ and β are positive but close to zero). Under these conditions, the evolution of the pathogen will be largely determined by reservoir dynamics that do not contribute to R_0 (eq. [3]). Although λ (eq. [2]) incorporates the growth of pathogens in the reservoir, it omits the effect of density dependence in the reservoir and consequently may be an inadequate fitness proxy when the reservoir initially harbors a pathogen population. In this case, a suitable fitness metric for studying long-term evolution is the invasion fitness, defined as the per capita growth rate of the mutant strain in a resident population that has reached its ecological/epidemiological attractor (Metz et al. 1996; Lion and Metz 2018). For facultative pathogens, the invasion fitness should be derived when the system has reached both epidemiological (endemic equilibrium) and ecological (nonzero equilibrium of free-living pathogen population in the reservoir) attractors. The next-generation matrix approach provides a biologically intuitive framework to derive the invasion fitness for organisms with multiple transmission routes or stage-structured life histories (Hurford et al. 2010). Thus, we use this framework to perform evolutionary invasion analysis in the following sections.

Evolutionary Invasion Analysis

Whenever $\lambda > 1$, system (1) goes to the endemic equilibrium ($\hat{S} > 0, \hat{I} > 0, \hat{P} > 0$). We chose parameter values such that there exists a locally stable endemic equilibrium (appendix, sec. A4) with positive numbers of individuals (appendix, sec. A3). The individual expressions for $\hat{S}, \hat{I}$, and $\hat{P}$ have many terms, so we do not present explicit expressions for these equilibria. In the following sections, we address

the outcome of long-term evolution when virulence trades off with other traits that impact fitness.

Case 1: Transmission-Virulence Trade-Off

We evaluated how a trade-off between direct transmission and virulence influences the virulence evolution of a facultative pathogen. We consider the case where the direct transmission rate is a saturating function of virulence, $\beta(\alpha) = c\alpha/(c\alpha + h)$. The invasion fitness of a mutant trait α_m in an environment set by the resident trait α is derived as the maximum eigenvalue of the next-generation matrix (eq. [A5.6]) for the mutant subsystem (appendix, sec. A5). Assuming a transmission-virulence trade-off, we obtain the following invasion fitness:

$$W(\alpha_m, \alpha) =$$
$$1 + \left(s_d \frac{\partial}{\partial \alpha_m} \left(\frac{\beta(\alpha_m)}{d + \rho + \alpha_m} \right) \right.$$
$$\left. + s_s \theta \frac{\partial}{\partial \alpha_m} \left(\frac{1}{d + \rho + \alpha_m} \right) \right)\Bigg|_{\alpha_m = \alpha} (\alpha_m - \alpha). \quad (6)$$

Here,

$$s_d = \frac{\theta}{d + \rho + \alpha} \frac{\gamma \hat{S}}{\sigma(1 + \hat{P})} \hat{S}$$

and

$$s_s = \left(1 - \frac{\beta \hat{S}}{d + \rho + \alpha} \right) \frac{\gamma \hat{S}}{\sigma(1 + \hat{P})},$$

where s_d describes the lifetime fitness gain from an infected host due to new infections and s_s describes the lifetime fitness gain from an infected host due to shedding of environmental propagules. Both s_s and s_d are proportional to the product of the elements of the left and right eigenvectors of the next-generation matrix. The left eigenvector is composed of the reproductive values of an infected host and an environmental propagule. The right eigenvector is composed of the equilibrium number of infected hosts and free-living propagules (appendix, sec. A5; Hurford et al. 2010). In the case of s_d, $\theta/(d + \rho + \alpha)$ is the scaled lifetime reproductive value of an infected host and $\gamma \hat{S}/(\sigma(1 + \hat{P}))$ is the scaled equilibrium population of infected hosts. Similarly, in the case of s_s, $(1 - \beta \hat{S}/(d + \rho + \alpha))$ is the scaled lifetime reproductive value of free-living pathogens. The partial derivatives within equation (6) are the fitness gradients that determine the direction of virulence evolution. A mutant pathogen with a higher virulence than the resident pathogen population ($\alpha_m > \alpha$) can invade the resident population if the sum of the scaled fitness gradients is positive. Similarly, if $\alpha_m < \alpha$, then the mutant can invade if the sum of scaled fitness gradients is negative.

In equation (6), the first fitness gradient represents fitness gain due to increased transmission, whereas the second fitness gradient,

$$\frac{\partial}{\partial \alpha_m} \left(\frac{1}{d + \rho + \alpha_m} \right),$$

is negative and thus represents fitness loss due to increased virulence. Higher virulence reduces the duration of infection, which consequently reduces the duration during which pathogen is shed into the reservoir. An intermediate-virulence evolutionarily stable strategy (ESS) occurs if the fitness gain due to increased transmission can more than compensate the fitness loss due to the reduction in shedding (e.g., strong transmission-virulence relationship; fig. 3b). Otherwise, low virulence is expected (fig. 3a). Since we are assuming that the virulence does not impact traits relevant to the reservoir, there is no variation in performance of the pathogen in the reservoir for the selection to act. Consequently, the ESS is independent of shedding rate (θ) and death rate (σ).

Case 2: Shedding-Virulence Trade-Off

Under the assumption where the shedding rate is a monotonically increasing function of virulence (i.e., $\theta(\alpha) = g\alpha/(g\alpha + f)$), the invasion fitness is given as

$$W(\alpha_m, \alpha) =$$
$$1 + \left(s_d \beta \frac{\partial}{\partial \alpha_m} \left(\frac{1}{d + \rho + \alpha_m} \right) \Bigg|_{\alpha_m = \alpha} \right.$$
$$\left. + s_s \frac{\partial}{\partial \alpha_m} \left(\frac{\theta(\alpha_m)}{d + \rho + \alpha_m} \right) \Bigg|_{\alpha_m = \alpha} \right) (\alpha_m - \alpha). \quad (7)$$

Here, the fitness gradient term has the same functional form as in case 1. Since the terms before the fitness gradients are proportional to the product of reproductive values and equilibrium populations, they have positive values. Hence, it also results in an intermediate ESS if the shedding and virulence are under a strong trade-off, while avirulence or low virulence is the outcome for a weak trade-off relationship.

If we assume that both transmission-virulence and shedding-virulence trade-offs exist for a given pathogen, then the outcome of evolution is determined by the combined fitness gradients from cases 1 and 2. Under these trade-off relationships, both fitness gradients point toward an intermediate ESS (fig. 4). However, if the shedding per generation and transmission per generation are maximized at different levels of virulence, then the outcome will be
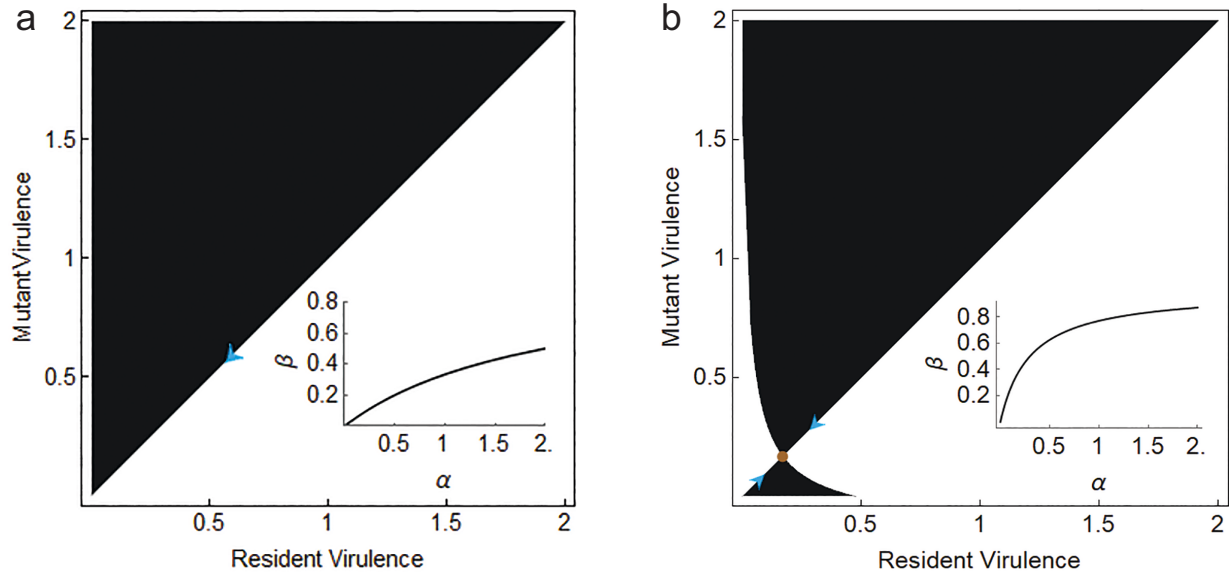
Figure 3: Pairwise invasibility plots showing virulence evolutionary outcomes where there is a trade-off between transmission and virulence. The shaded region shows the area where the invasion fitness is less than 1 (i.e., mutant cannot invade), whereas the white region shows the area where the invasion fitness is greater than 1. Arrows indicate the direction of trait evolution. *a*, With a weak trade-off (shown in the inset; $h = 2$), the pathogen evolves toward avirulence. *b*, For a stronger transmission-virulence trade-off ($h = 0.3$), intermediate virulence (brown circle) is expected, as shown. Parameter values: $c = 1$, $\theta = 0.2$, $\sigma = 0.05$, $\tau = 1$, $K = 15$.
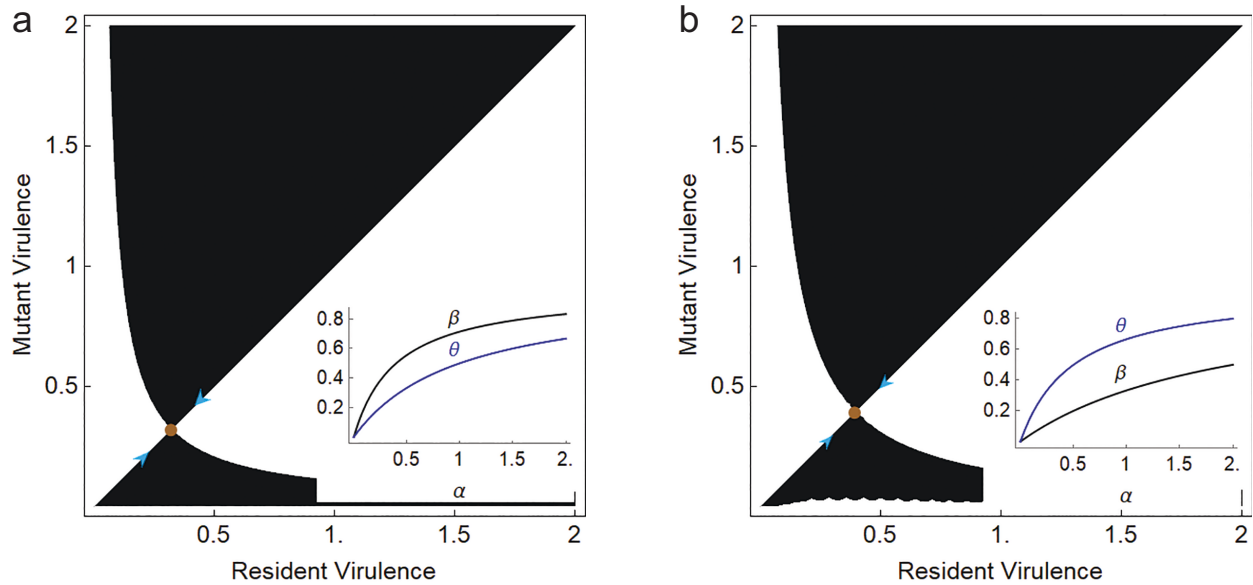

Figure 4: Pairwise invasibility plots showing virulence outcomes for combined transmission-virulence and shedding-virulence trade-offs. Arrows indicate the direction of trait evolution. *a*, Intermediate evolutionarily stable strategy (ESS) results with strong transmission-virulence trade-off (black line in inset; $h = 0.4$) and weak shedding-virulence trade-off (blue line in inset; $f = 1$). *b*, Similar intermediate ESS results with strong shedding-virulence trade-off ($f = 0.5$) and weak transmission-virulence trade-off ($h = 2$). All other parameters are the same as in figure 3.

determined by the relative fitness effects of shedding and transmission.

Case 3: Free-Living Pathogen Persistence-Virulence Trade-Off

The distinctive feature of facultative pathogens is their potential for host-independent growth and survival. We have decomposed the birth and death rate of free-living pathogens in the reservoir in system (1). Adaptation toward the reservoir environment can come in at least two different forms: increase in birth rate or decrease in death rate (increase in persistence). Because system (1) has density-dependent birth rates, for simplicity we consider the case of selection to reduce the death rate, thereby increasing the period of time that environmental propagules persist in the reservoir ($1/\sigma$). The invasion fitness in this case can be written as

$$W(\alpha_m, \alpha) =$$
$$1 + \left(s_d \beta \frac{\partial}{\partial \alpha_m} \left(\frac{1}{d + \rho + \alpha_m} \right) \right.$$
$$+ s_s \theta \frac{\partial}{\partial \alpha_m} \left(\frac{1}{d + \rho + \alpha_m} \right) \tag{8}$$
$$\left. + s_e \frac{\partial}{\partial \alpha_m} \left(\frac{1}{\sigma(\alpha_m)} \right) \right) \Big|_{\alpha_m = \alpha} (\alpha_m - \alpha).$$

Here,

$$s_e = \left(1 - \frac{\beta \hat{S}}{d + \rho + \alpha} \right) \frac{\theta}{d + \rho + \alpha} \frac{\gamma \hat{S}}{(1 + \hat{P})}$$
$$+ \left(1 - \frac{\beta \hat{S}}{d + \rho + \alpha} \right)^2 r \left(1 - \frac{\hat{P}}{K} \right)$$

and represents the lifetime contribution due to free-living pathogens. The first term,

$$\left(1 - \frac{\beta \hat{S}}{d + \rho + \alpha} \right) \frac{\theta}{d + \rho + \alpha} \frac{\gamma \hat{S}}{(1 + \hat{P})},$$

gives the lifetime contribution of free-living pathogens to new infections, whereas the second term,

$$\left(1 - \frac{\beta \hat{S}}{d + \rho + \alpha} \right)^2 r \left(1 - \frac{\hat{P}}{K} \right),$$

gives the lifetime contribution of free-living pathogens toward growth in environmental reservoir. Depending on the exact mechanisms involved, two different functional relationships between pathogen persistence and virulence can be considered. For the first case, we consider a positive correlation between persistence and virulence. The selection gradient associated with s_e represents fitness gain due to increased persistence, whereas selection gradients associated with s_d and s_s represent fitness losses due to increased virulence and shorter duration of infection. The result of evolution then depends on the balance of these opposing selection gradients. Bistability is observed for some parameter values, and the attained ESS virulence depends on the initial virulence level (fig. 5a). If the initial virulence level is low, it pays for the pathogen to have lower virulence because of the benefit of increased duration of infection. However, if the initial virulence starts above the trait value of the repeller point (red circle in fig. 5a), increased persistence more than compensates for the fitness loss due to increased virulence. Consequently, virulence evolves to higher levels (figs. 5a, S5; figs. S1–S6 are available online).

We also consider a different functional relationship between persistence and virulence where the increase in virulence leads to lowering of pathogen persistence. Specifically, we assume the functional form $\sigma(\alpha) = a/(e^{-u\alpha} + v)$, where a, u, and v are positive constants. Here, all three fitness gradients have the same sign such that it is beneficial for the pathogen to have both a low death rate in the reservoir and low virulence because of the fitness benefits. Consequently, avirulence is the expected outcome for this form of virulence-persistence relationships (figs. 5b, S5).

Case 4: Multiple Trade-Offs

Although the outcomes of evolution can be easily determined for single trade-offs, systems with multiple trade-offs can have more diverse evolutionary outcomes. For some pathogens, it is likely that virulence is correlated with traits that determine fitness both within hosts and in the reservoir. The outcome of virulence evolution then depends on the selection gradients acting in these environments. To explore potential outcomes, we start by considering both transmission-virulence and persistence-virulence trade-offs, followed by a scenario where we also include a relationship between virulence and shedding.

Case 4a: Combined Transmission-Virulence and Persistence-Virulence Trade-Off. The invasion fitness in this case is given as

$$W(\alpha_m, \alpha) =$$
$$1 + \left(s_d \frac{\partial}{\partial \alpha_m} \left(\frac{\beta(\alpha_m) \hat{S}}{d + \rho + \alpha_m} \right) \right.$$
$$+ s_s \theta \frac{\partial}{\partial \alpha_m} \left(\frac{1}{d + \rho + \alpha_m} \right) \tag{9}$$
$$\left. + s_e \frac{\partial}{\partial \alpha_m} \left(\frac{1}{\sigma(\alpha_m)} \right) \right) \Big|_{\alpha_m = \alpha} (\alpha_m - \alpha).$$

Assuming that both transmission and pathogen persistence are positively correlated with virulence, the selection gradient associated with s_d represents the fitness benefit associated
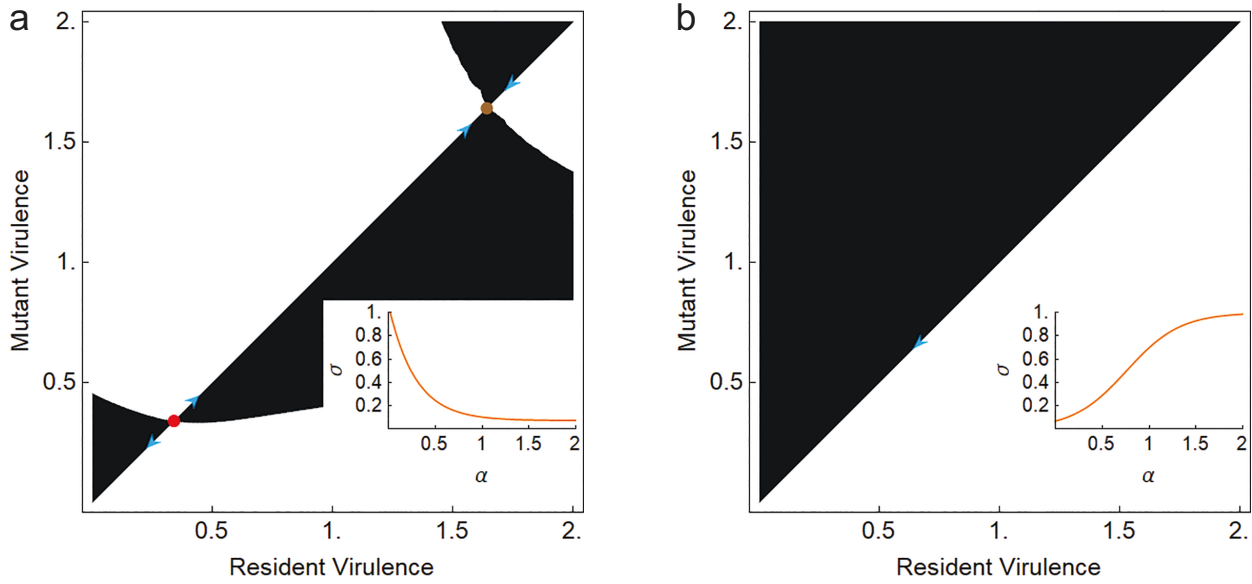
Figure 5: Pairwise invasibility plots for virulence evolution under persistence-virulence trait correlation. Arrows indicate the direction of trait evolution. *a*, Persistence-virulence trade-off ($\sigma(\alpha) = e^{-u\alpha} + v$; i.e., the death rate in the environment decreases with increasing virulence) results in bistability conditions separated by a repeller (red circle) where the evolutionarily stable strategy (brown circle) depends on the initial condition for virulence. Parameter values: $b = 2$, $\beta = 0.12$, $\theta = 0.3$, $r = 0.3$, $u = 3.5$, $v = 0.07$, $\tau = 1$. *b*, Positive correlation between virulence and death rate ($\sigma(\alpha) = a/(e^{-u\alpha} + v)$) results in evolution toward avirulence. Parameter values: $a = 0.07$, $u = 3.5$, $v = 0.07$. All other parameters are the same as in previous figures.

with increased transmission, s_s represents the fitness cost associated with increased virulence (decreased duration for shedding), and s_e represents the fitness benefit associated with increased persistence. When initial virulence levels are low, fitness gradients associated with both transmission and persistence point toward higher virulence. An opposing selection gradient is associated with shedding, which points toward lower virulence. ESS virulence occurs whenever the three weighted selection gradients are balanced. If the virulence is too high, the fitness benefit due to increased transmission and persistence does not compensate for the fitness loss due to increased virulence.

Case 4b: Virulence-Transmission, Virulence-Shedding, and Virulence-Persistence Trade-Offs. In this section, we consider scenarios where all three trade-offs explored above are present. The invasion fitness for this case can be written as

$$W(\alpha_m, \alpha) =$$
$$1 + \left(\left(s_d \frac{\partial}{\partial \alpha_m} \left(\frac{\beta(\alpha_m)}{d + \rho + \alpha_m} \right) \right. \right.$$
$$+ s_s \frac{\partial}{\partial \alpha_m} \left(\frac{\theta(\alpha_m)}{d + \rho + \alpha_m} \right) \tag{10}$$
$$\left. \left. + s_e \frac{\partial}{\partial \alpha_m} \left(\frac{1}{\sigma(\alpha_m)} \right) \right) \right) \bigg|_{\alpha_m = \alpha} (\alpha_m - \alpha).$$

The three weighted fitness gradients determine the direction of selection on virulence. Singular points occur whenever the sum of all fitness gradients weighted by their respective reproductive values is zero. This can be achieved because of the trade-offs, such that selection gradients act in opposite directions with respect to the trait and the fitness contribution obtained by changing the trait in one term is cancelled by the fitness change in another term. If we assume a positive correlation between virulence and persistence, then

$$\frac{\partial}{\partial \alpha_m} \left(\frac{1}{\sigma(\alpha_m)} \right) \geq 0.$$

In this case, no singular strategies exist where virulence increases both transmission and shedding. Singular strategies can exist when there is a positive relationship between virulence and persistence if

$$s_d \frac{\partial}{\partial \alpha_m} \left(\frac{\beta(\alpha_m)}{d + \rho + \alpha_m} \right) + s_s \frac{\partial}{\partial \alpha_m} \left(\frac{\theta(\alpha_m)}{d + \rho + \alpha_m} \right) < 0.$$

We can explore different possibilities by changing the strength of trade-offs. For example, if we keep the strength of the transmission-virulence and shedding-virulence trade-offs constant, then increasing the strength of the trade-off between persistence and virulence leads to lower virulence (fig. 6). A simple comparison between the results in the
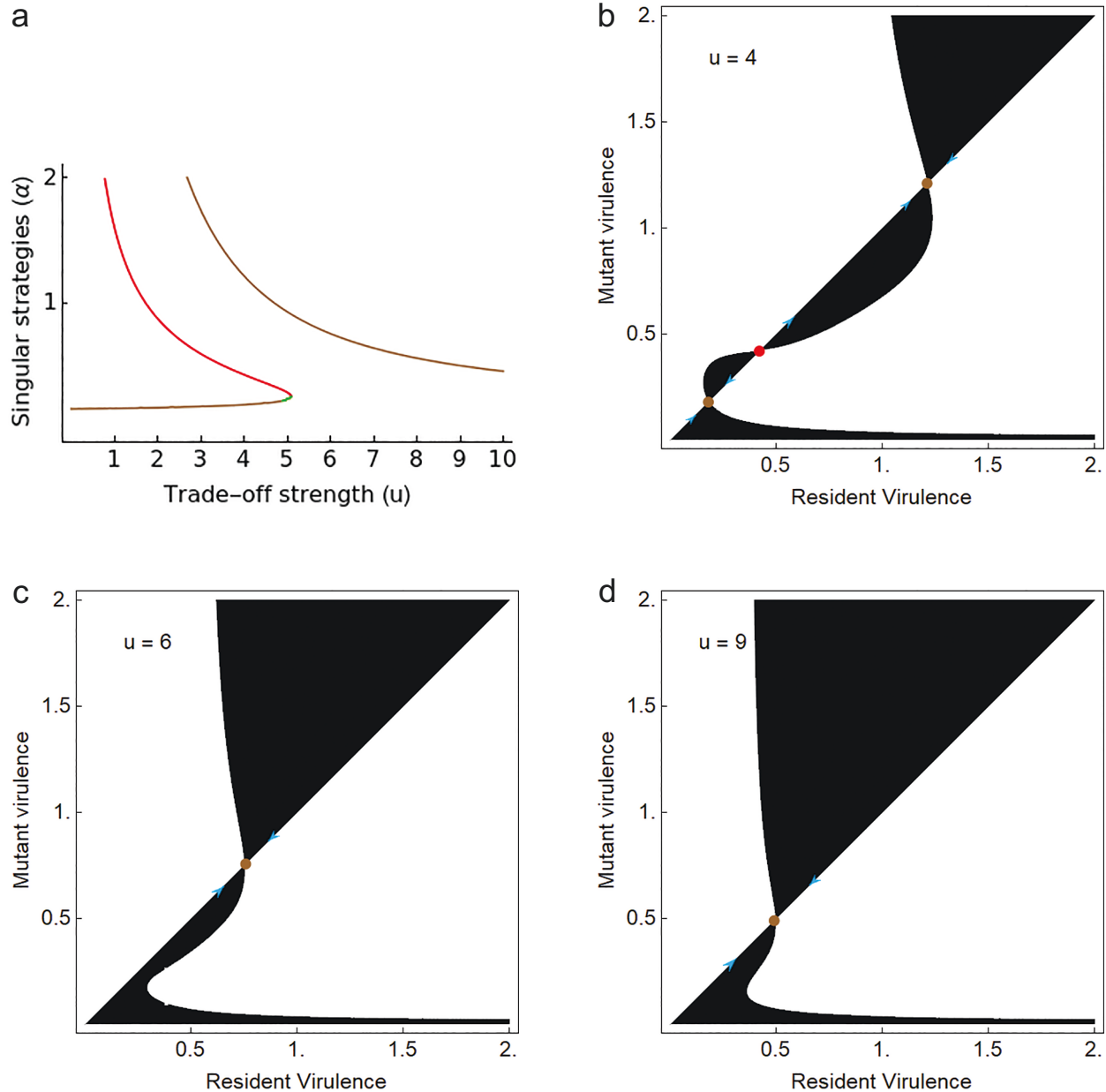
Figure 6: Virulence evolution with multiple trade-offs. *a*, Bifurcation diagram with singular strategies as a function of *u*, which determines the shape of the relationship between environmental persistence and virulence. Brown lines indicate evolutionarily stable strategies (ESSs), whereas the red and green lines represent repellers and evolutionary branching points, respectively. *b–d*, Pairwise invasibility plots with different values of *u*. Brown circles represent ESSs, and red points indicate repeller points. Arrows indicate the direction of trait evolution. Parameter values: $v = 0.02$, $g = 1$, $f = 1$, $c = 1$, $h = 0.1$, $K = 15$, $r = 0.07$, $\tau = 1$.

figure 6 and that in Boldin and Kisdi (2012) shows that the addition of growth in the reservoir increases the value of singular strategies. Bistability is observed for a wide range of (*u*) values (fig. 6*a*), where the final ESS attained is dependent on the virulence of the initial strain. Depending on the strength of the trade-offs in the system, singular strategies can become evolutionary branching points where patho-

gens with both low and high virulence can coexist (compare fig. 7*c* and fig. 8).

Case 4c: Effect of Carrying Capacity. Several factors, such as a change in environmental conditions or competitor populations, can change the carrying capacity of the pathogen's reservoir populations. While we have not assumed any
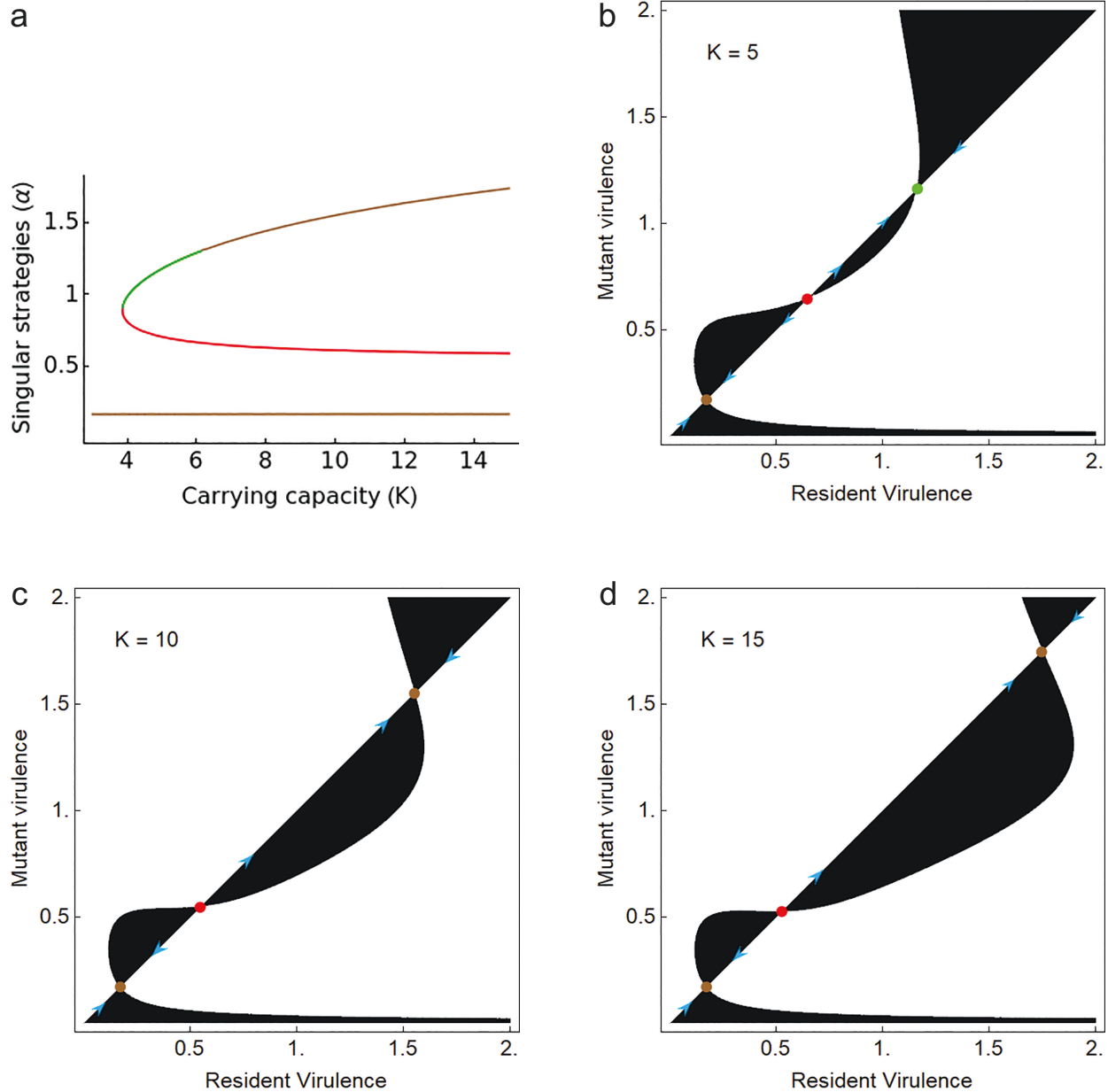
Figure 7: Effect of reservoir carrying capacity on virulence evolutionary outcomes. *a*, Bifurcation plot with singular strategies as a function of carrying capacity (K). Brown lines indicate evolutionarily stable strategies (ESSs), whereas the red and green lines represent repellers and evolutionary branching points, respectively. The upper ESSs increase with increasing K. *b*–*d*, Pairwise invasibility plots with different values of K. Brown circles indicate ESSs, red circles represent repellers, and the green circle represents an evolutionary branching point. Arrows indicate the direction of trait evolution. Parameter values: $v = 0.02$, $g = 1$, $f = 1$, $c = 1$, $h = 0.1$, $\alpha = 1$, $r = 0.1$, $u = 3$, $\tau = 1$.

correlation between virulence and the reservoir carrying capacity, a change in carrying capacity can still impact the direction of virulence evolution by changing the scaling factor s_e in equation (8). Our results suggest that as the reservoir becomes more favorable for the pathogens by increasing the carrying capacity, we expect the evolution of higher virulence. Similarly, increased carrying capacity also increases the disease prevalence (fig. 2*b*). High carrying capacity can

lead to high equilibrium pathogen population size in the reservoir, which can then increase the number of infections.

Critical Function Analysis

The simulation results presented so far assume specific trade-off forms (e.g., fig. 3). Critical function analysis (de Mazancourt and Dieckmann 2004; Kisdi 2006) provides the
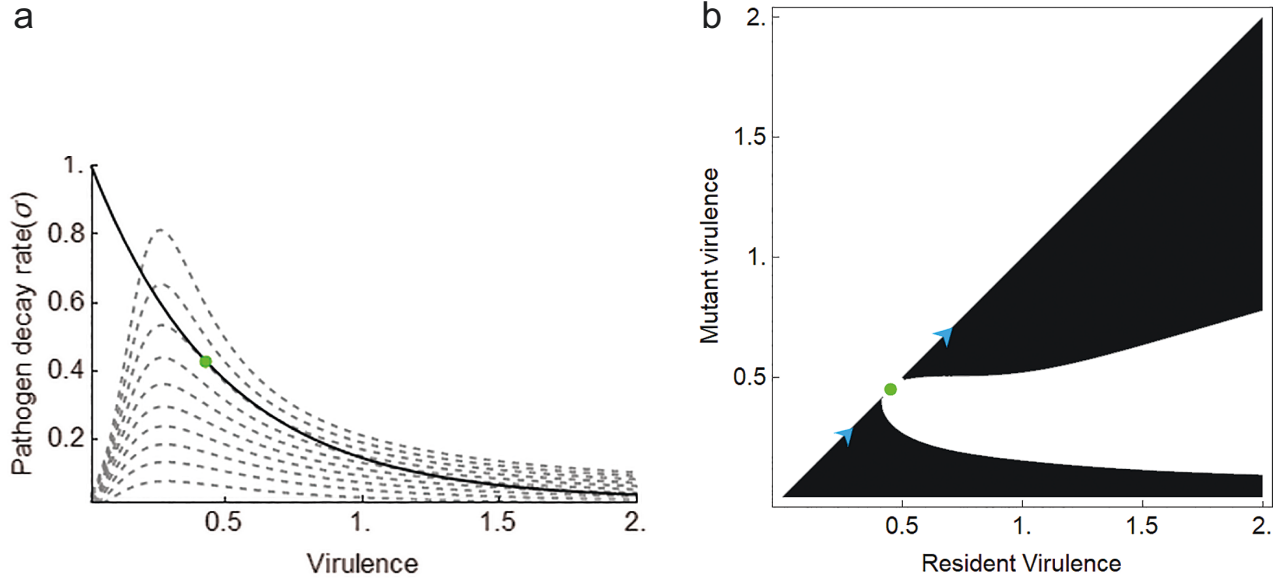
a

b

Figure 8: Critical function analysis and the nature of singular strategies. *a*, Dashed curves represent critical functions that are numerical solutions of equation (12) with different initial conditions. The black solid line represents the persistence-virulence trade-off ($u = 2.1$). The green circle represents the singular strategy where the trade-off is tangent to the critical function. *b*, The singular strategy obtained in *a* is convergence stable but evolutionarily unstable, thus leading to an evolutionary branching point (green circle in pairwise-invasibility plot). Arrows indicate the direction of trait evolution. Parameter values are the same as in figure 7*c*, except $h = 0.3$.

framework to generalize the results that are independent of specific trade-off assumptions. Scenarios involving a single trade-off are straightforward (see the appendix, sec. A7). Here, we focus on multiple trade-offs considered in figure 6 (fig. 8), with additional scenarios presented in the appendix (sec. A7; figs. S5, S6).

From equation (10), singular strategies are obtained when

$$\left(s_d \frac{\partial}{\partial \alpha_m} \left(\frac{\beta(\alpha_m)}{d + \rho + \alpha_m} \right) + s_s \frac{\partial}{\partial \alpha_m} \left(\frac{\theta(\alpha_m)}{d + \rho + \alpha_m} \right) \right.$$
$$\left. + s_e \frac{\partial}{\partial \alpha_m} \left(\frac{1}{\sigma(\alpha_m)} \right) \right) \Bigg|_{\alpha_m = \alpha} = 0.$$

(11)

If the shapes of all three trade-offs are unknown, equation (11) is underdetermined. Building on the analysis presented in the section on case 4b, we fix the shape of transmission-virulence and shedding-virulence trade-offs and assume a general relationship for the persistence-virulence trade-off. This gives us the following differential equation:

$$\sigma'_{\text{crit}}(\alpha) = \left(\frac{\sigma^2_{\text{crit}}(\alpha)}{s_e} \right)$$
$$\times \frac{(s_d((d + \rho + \alpha)\beta'(\alpha) - \beta(\alpha)) + s_s((d + \rho + \alpha)\theta'(\alpha) - \theta(\alpha)))}{(d + \rho + \alpha)^2},$$

(12)

where, $\sigma_{\text{crit}}(\alpha)$ is a critical function. The solutions of equation (12) with different initial conditions result in a family

of critical functions (e.g., fig. 8*a*). Singular points are obtained whenever the trade-off is tangent to the critical function. Convergence stability of the singular points is determined by the local shape of the trade-off. If the trade-off is more concave than the critical function, the singular point is convergence stable (see fig. 8*a* and the appendix, sec. A7). Convergence stability along with the nature of evolutionary stability determine the type of singular strategies possible. For example, in figure 8*b* the singular strategy is convergence stable but evolutionarily unstable and thus results in an evolutionary branching point (fig. 8*b*).

Discussion

The selective pressures shaping the evolution of virulence depend on the pathogen's life history and the fitness trade-offs the pathogen faces. Many pathogens can be environmentally transmitted from and reproduce within reservoir environments. The fitness of these pathogens depends on how well they perform functions associated with infecting hosts as well as selective pressures imposed in environmental reservoirs. Evolutionary responses to these selective pressures can have significant consequences for how facultative pathogens interact with hosts, particularly when virulence factors have additional functions in reservoir environments.

Stage-structured life histories of pathogens may diminish the role of a trade-off between virulence and transmission

but may pose alternative fitness trade-offs shaping the evolution of virulence. The importance of different types of constraints on virulence evolution due to heterogeneous environments has already studied in the context of multihost parasite systems (Regoes et al. 2000; Gandon 2004). Environmental transmission of dormant environmental propagules (e.g., spores or virions) may allow pathogens to partly circumvent a potential transmission-virulence trade-off, allowing for higher virulence (Gandon 1998; Day 2002b; Boldin and Kisdi 2012). Consistent with these theoretical predictions, waterborne pathogens, which primarily infect hosts from environmental reservoirs, are highly virulent (Ewald 1991b; Walther and Ewald 2004; Pulkkinen et al. 2010; Breban 2013; Kinnula et al. 2017).

Pathogen growth in environmental reservoirs provides abundant opportunities for ecological trade-offs stemming from traits that are beneficial in one environment being detrimental in another (Sokurenko et al. 2006; Caraco and Wang 2008; Brown et al. 2012; Friman et al. 2013; Martínez 2014; Mikonranta et al. 2015; Barton et al. 2018). We explored the consequences of a potential trade-off between virulence and persistence, virulence and transmission, and virulence and shedding on the evolution of facultative pathogen virulence. When considered in isolation, each trade-off predicts intermediate to high virulence provided that the fitness gain from increased virulence in correlated traits more than compensates for the fitness loss due to reduced duration of infection (increased virulence; figs. 3a, 4a, 5a). This occurs when there are strong trade-offs, such that a slight increase in virulence leads to a large change in the correlated trait (transmission, shedding, or persistence).

The life history of facultative pathogens and its inherent heterogeneous selection may result in multiple simultaneous trade-offs associated with virulence. Based on qualitative analysis of the conditions under which the invasion fitness (eq. [10]) equals 1, at least one singular strategy is possible only when one fitness gradient associated with direct transmission, shedding, or environment persistence is of opposite sign relative to the others. With multiple trade-offs, bistability and evolutionary branching points occur over a wide range of parameter values (figs. 6a, 7a). Evolutionary bistability occurs when a monomorphic population can evolve to either low virulence or high virulence depending on the virulence of the initial population. Bistability occurs even with a single trade-off between persistence and virulence (fig. 5a). Branching points occur when any monomorphic population starting on either side of the branching point will converge toward this point. However, once the population reaches the branching point, disruptive selection results in a dimorphic population. The long-term fate of each subpopulation depends on the invasion fitness of each phenotype in the dimorphic population (Geritz et al. 1998). We observe that evolutionary branching is possible for fac-

ultative pathogens (figs. 6a, 7a), in part depending on the strength of the trade-offs in the system (e.g., compare fig. 7c and fig. 8). Consistent with the idea that diverse virulence strategies may be likely in pathogens with heterogeneous selection and environmental transmission, Boldin and Kisdi (2012) also identified bistability and branching outcomes for a wide parameter range in their model.

The relationship between the virulence and growth rate of pathogens in the reservoir is likely context dependent and variable among facultative pathogens. In some cases, there may be preadaptation or coincidental selection such that the pathogen's growth rate in the reservoir is positively correlated with virulence (Levin 1996; Brown et al. 2012; Sundberg et al. 2016). This may be true when virulence factors also play a role in promoting survival in the environmental reservoir. For example, in an emerging opportunistic human pathogen *Stenotrophomonas maltophilia*, a type IV secretion system is involved in both competition against heterologous bacteria and apoptosis of human macrophages (Bayer-Santos et al. 2019; Nas et al. 2019). Competition in environmental reservoirs can impose strong selection pressure to maintain these molecular machineries, which can then be co-opted for other functions, such as secretion of virulence factors. Similar correlations between pathogen survival in reservoirs and virulence occurs in Shiga toxin–producing pathogens, where Shiga toxin provides resistance against grazers and increases host damage (Steinberg and Levin 2007; Adiba et al. 2010). Consistent with these observations, our model predicts that a positive correlation between environmental persistence and virulence results in high ESS virulence (fig. 5a).

Alternatively, specialized mechanisms may be required for survival and resource acquisition of the pathogen in host and reservoir environments. This may result in a negative correlation between growth/survival in the reservoir and virulence (Kaitala et al. 2017). As an example, evolution of phage resistance—essential to environmental persistence—has been shown to reduce virulence in *Listeria monocytogenes* (Sumrall et al. 2019). In this study, phage resistance mediated by modifications of *L. monocytogenes* O antigen results in lower invasiveness of mammalian cells and in vivo virulence attenuation in mice. When increased virulence is associated with lower environmental persistence, our model predicts a decrease in virulence (fig. 5b). This is consistent with the empirical observation where the evolution of increased environmental persistence via antipredator adaptation results in reduced virulence of *Serratia marcescens* (Mikonranta et al. 2012). Similarly, the evolution of phage resistance also resulted in the reduction of virulence in a fish pathogen, *Flavobacterium columnare* (Laanto et al. 2012). For these reasons, the functional relationship between virulence and traits affecting performance in the reservoir are required to predict the evolution of virulence.

In addition to the effects of varying trade-offs, other environmental parameters can potentially change both epidemiological and evolutionary outcomes. Our results suggest that the endemic prevalence of disease is more sensitive to reservoir carrying capacity than to the effect of free-living pathogen birth rate (fig. 2b). Reservoir carrying capacity depends on abiotic (e.g., nutrients, temperature) and biotic (e.g., competition, parasitism, predation) factors and has been shown to influence epidemiological outcomes for environmentally growing opportunistic pathogens (Anttila et al. 2013, 2016; Kaitala et al. 2017; Merikanto et al. 2018). We also explored the evolutionary consequences for virulence of varying reservoir carrying capacities while keeping the strength of trade-offs constant. In general, increasing the carrying capacity in the environmental reservoir can increase a facultative pathogen's evolutionarily stable virulence strategy (fig. 7), suggesting that the higher carrying capacity can offset the fitness cost of increased virulence. This result is similar to the prediction from multihost systems that increased fitness in one host can compensate for the fitness cost associated with increased virulence affecting a second host (Gandon 2004). When carrying capacity is relatively low, our results suggest possible evolutionary diversification indicated by the evolutionary branching points (fig. 7a, 7b). Interestingly, a long-term evolution experiment of *F. columnarae* under low nutrient conditions resulted in the diversification of morphotypes with varying virulence (Sundberg et al. 2014). In contrast, the evolution of *F. columnarae* under high nutrient conditions in the reservoir results in higher virulence (Kinnula et al. 2017), which is consistent with our predictions for increasing the carrying capacity (fig. 7b–7d).

The adaptive dynamics framework relies on the assumption of specific trade-off shapes. However, the empirical determination of the exact shape of trade-off is often difficult (Ebert and Bull 2003; Alizon et al. 2009; Alizon and Michalakis 2015). Although we have assumed qualitatively different trait correlations in some of the results (e.g., fig. 5a, 5b), more general results are obtained through geometric analyses that are independent of specific trade-off shapes (de Mazancourt and Dieckmann 2004; Kisdi 2006). We used critical function analysis to assess the location and nature of singular strategies in the trait space (figs. 8, S5, S6). A singular strategy occurs when the critical function is tangent to the trade-off function. With multiple trade-offs, it is possible to get a singularity of an arbitrary type given enough environmental feedbacks (Kisdi 2015). To avoid this, we fix some of the trade-off shapes and explore outcomes for others. For example, we fixed the shape of the transmission-virulence and shedding-virulence trade-offs to get an explicit differential equation of the critical function related to the trait correlation of pathogen decay rate and virulence (eq. [12]). Numerical solutions of this equation and invasion analysis show that stronger negative correlations between pathogen decay rate and virulence can result in lower virulence singular traits than weaker negative correlations (figs. 6, 8a). However, unlike the case of a single trait correlation (fig. S5), a nonzero singular trait is possible even for a positive correlation between the pathogen decay rate and virulence. Similar analysis can be performed for transmission-virulence or shedding-virulence trait correlations if the shapes of the remaining two trait correlations are fixed (see the appendix, sec. A7).

Facultative pathogens pose a challenge to the determination and interpretation of the basic reproduction number (R_0)—an important threshold parameter used to evaluate potential epidemiological and evolutionary outcomes. The next-generation matrix method provides an intuitive approach for deriving R_0 of different systems. There are different ways to construct the next-generation matrix for the same system, but how we structure the next-generation matrix changes the biological interpretation of the threshold parameter obtained. Although many of these have the same threshold properties as R_0 (e.g., Bani-Yaghoub et al. 2012), not all threshold parameters obtained from the next-generation matrices follow the strict definition of the epidemiological R_0. If the objective is to purely look at the disease outcomes by deciding whether the disease dies out or leads to an outbreak, then all of the R_0-like threshold parameters derived from different next-generation matrix considerations behave equivalently (appendix, sec. A2). However, if the objective is to quantify the contribution of a single infected individual to secondary infections, then the R_0 is needed. The conventional method of deriving the R_0 as the maximum eigenvalue of the next-generation matrix leads to a threshold metric quantitatively different from the epidemiological R_0. Unlike Boldin and Kisdi (2012), our model has two "birth" types in the "transmission matrix." When there is more than one type of birth in the transmission matrix component of the next-generation matrix, there is an important distinction between the demographic reproduction number (which we refer to as λ in the results section) and the epidemiological reproduction number (R_0), as these parameters represent two fundamentally different biological quantities and, hence, can have different magnitudes. Thus, we provide a general recipe for R_0 derivation and explain its difference with the demographic threshold parameter λ. The advantage of using this technique to determine the R_0 is that it is easier to interpret than other threshold expressions and allows us to decompose the contribution of each transmission route to new infections.

For many pathogens, the epidemiological R_0 can be a suitable fitness proxy to study virulence evolution. However, since the epidemiological R_0, by definition, is focused on disease transmission to the hosts, it omits the free-living pathogen growth dynamics in the reservoir. A better fitness metric should ideally close the life cycle of pathogens (Alizon and Michalakis 2015). For this reason, the demographic reproduction

number (λ) better describes facultative pathogen dynamics than R_0. However, because λ is derived under the assumption of no initial free-living pathogens in the reservoir, it is only a suitable fitness metric when the pathogen is initially absent in the reservoir. Consequently, because the invasion fitness is derived when both the host and the free-living pathogen population reach equilibrium, it is a better fitness metric than λ and R_0 because it incorporates the effect of density dependence in the reservoir.

The life history of facultative pathogens features distinct population dynamics occurring in environmental reservoirs and during transmission to hosts and can involve multiple transmission routes. Our model extends the model from Boldin and Kisdi (2012) in order to explore consequences of preadaptation and coincidental selection in reservoirs for facultative pathogens. We further explored the consequences of parameters relevant to reservoir dynamics (e.g., reservoir carrying capacity, free-living pathogen growth rate) to disease dynamics and virulence evolution. However, we deliberately kept the model simple to maintain tractability and facilitate interpretation. Although a positive correlation between the pathogen's birth rate in the reservoir and virulence is possible, density dependence with birth rate makes calculations required to explore this trade-off cumbersome. Thus, we restricted our analysis to a simpler correlation between the pathogen's reservoir death rate and virulence. We also neglected potential interactions of free-living propagules with other organisms in the reservoir. Bacterial competitors and predators can potentially influence the trait dynamics in the reservoir (Godfray et al. 1999; Friman et al. 2009).

Many facultative pathogens are of public health, economic, and ecological importance. Despite this, the consequences of such life histories on virulence evolution have often been overlooked in previous studies. Although our model is a simplification of facultative pathogen life history, the alignment of qualitative model predictions with several empirical observations is encouraging. These empirical agreements are, however, merely correlative suggestions, and hence future work connecting modeling and experiment is required to establish the selective pressures determining the evolution of facultative pathogen virulence. Empirical work evaluating the trade-offs faced by facultative pathogens is required for a comprehensive theory of virulence evolution capable of predicting how virulence evolves in these systems.

Statement of Authorship

T.G.P., N.M., and A.P. were responsible for conceptualization. T.G.P. and N.M. acquired funding. A.P. performed model analysis and coding simulation. All authors wrote the manuscript.

Data and Code Availability

The Mathematica notebook with code for analysis and for figures is available at https://github.com/apandey101/facultative-pathogen-model and is archived at Zenodo (http://doi.org/10.5281/zenodo.4718509).

Literature Cited

Acevedo, M. A., F. P. Dillemuth, A. J. Flick, M. J. Faldyn, and B. D. Elderd. 2019. Virulence-driven trade-offs in disease transmission: a meta-analysis. Evolution 73:636–647.

Adiba, S., C. Nizak, M. van Baalen, E. Denamur, and F. Depaulis. 2010. From grazing resistance to pathogenesis: the coincidental evolution of virulence factors. PLoS ONE 5:e11882.

Alizon, S., A. Hurford, N. Mideo, and M. van Baalen. 2009. Virulence evolution and the trade-off hypothesis: history, current state of affairs and the future. Journal of Evolutionary Biology 22:245–259.

Alizon, S., and Y. Michalakis. 2015. Adaptive virulence evolution: the good old fitness-based approach. Trends in Ecology and Evolution 30:248–254.

Anderson, R. M., and R. M. May. 1978. Regulation and stability of host-parasite population interactions. I. Regulatory processes. Journal of Animal Ecology 47:219–247.

———. 1981. The population dynamics of microparasites and their invertebrate hosts. Philosophical Transactions of the Royal Society B 291:451–524.

Anttila, J., J. Laakso, V. Kaitala, and L. Ruokolainen. 2016. Environmental variation enables invasions of environmental opportunist pathogens. Oikos 125:1144–1152.

Anttila, J., L. Ruokolainen, V. Kaitala, and J. Laakso. 2013. Loss of competition in the outside host environment generates outbreaks of environmental opportunist pathogens. PLoS ONE 8:e71621.

Bani-Yaghoub, M., R. Gautam, Z. Shuai, P. van den Driessche, and R. Ivanek. 2012. Reproduction numbers for infections with free-living pathogens growing in the environment. Journal of Biological Dynamics 6:923–940.

Barton, I. S., C. Fuqua, and T. G. Platt. 2018. Ecological and evolutionary dynamics of a model facultative pathogen: *Agrobacterium* and crown gall disease of plants. Environmental Microbiology 20:16–29.

Bayer-Santos, E., W. Cenens, B. Y. Matsuyama, G. U. Oka, G. Di Sessa, I. D. V. Mininel, T. L. Alves, et al. 2019. The opportunistic pathogen *Stenotrophomonas maltophilia* utilizes a type IV secretion system for interbacterial killing. PLoS Pathogens 15: e1007651.

Boldin, B., and É. Kisdi. 2012. On the evolutionary dynamics of pathogens with direct and environmental transmission. Evolution 66:2514–2527.

Bonhoeffer, S., R. E. Lenski, and D. Ebert. 1996. The curse of the pharaoh: the evolution of virulence in pathogens with long living propagules. Proceedings of the Royal Society B 263:715–721.

Breban, R. 2013. Role of environmental persistence in pathogen transmission: a mathematical modeling approach. Journal of Mathematical Biology 66:535–546.

Brown, S. P., D. M. Cornforth, and N. Mideo. 2012. Evolution of virulence in opportunistic pathogens: generalism, plasticity, and control. Trends in Microbiology 20:336–342.

Caraco, T., and I. N. Wang. 2008. Free-living pathogens: life-history constraints and strain competition. Journal of Theoretical Biology 250:569–579.

Charnov, E. 1989. Phenotypic evolution under Fisher's fundamental theorem of natural selection. Heredity 62:113–116.

Codeço, C. T. 2001. Endemic and epidemic dynamics of cholera: the role of the aquatic reservoir. BMC infectious diseases 1:1.

Cressler, C. E., D. V. McLoed, C. Rozins, J. van den Hoogen, and T. Day. 2016. The adaptive evolution of virulence: a review of theoretical predictions and empirical tests. Parasitology 143:915–930.

Day, T. 2002a. The evolution of virulence in vector-borne and directly transmitted parasites. Theoretical Population Biology 62:199–213.

———. 2002b. Virulence evolution via host exploitation and toxin production in spore-producing pathogens. Ecology Letters 5:471–476.

de Mazancourt, C., and U. Dieckmann. 2004. Trade-off geometries and frequency-dependent selection. American Naturalist 164:765–778.

Diekmann, O., J. A. P. Heesterbeek, and M. G. Roberts. 2009. The construction of next-generation matrices for compartmental epidemic models. Journal of the Royal Society Interface 7:873–885.

Ebert, D., and J. J. Bull. 2003. Challenging the trade-off model for the evolution of virulence. Trends in Microbiology 11:15–20.

Ewald, P. W. 1983. Host-parasite relations, vectors, and the evolution of disease severity. Annual Review of Ecology and Systematics 14:465–485.

———. 1991a. Transmission modes and the evolution of virulence—with special reference to cholera, influenza, and AIDS. Human Nature 2:1–30.

———. 1991b. Waterborne transmission and the evolution of virulence among gastrointestinal bacteria. Epidemiology and Infection 106:83–119.

Frank, S. A. 1996. Models of parasite virulence. Quarterly Review of Biology 71:37–78.

Friman, V. P., M. Ghoul, S. Molin, H. K. Johansen, and A. Buckling. 2013. *Pseudomonas aeruginosa* adaptation to lungs of cystic fibrosis patients leads to lowered resistance to phage and protist enemies. PLoS ONE 8:e75380.

Friman, V. P., C. Lindstedt, T. Hiltunen, J. Laakso, and J. Mappes. 2009. Predation on multiple trophic levels shapes the evolution of pathogen virulence. PLoS ONE 4:e6761.

Gandon, S. 1998. The curse of the pharaoh hypothesis. Proceedings of the Royal Society B 265:1545–1552.

———. 2004. Evolution of multihost parasites. Evolution 58:455–469.

Geritz, S. A. H., É. Kisdi, G. Meszena, and J. A. J. Metz. 1998. Evolutionarily singular strategies and the adaptive growth and branching of the evolutionary tree. Evolutionary Ecology 12:35–57.

Godfray, H. C. J., C. J. Briggs, N. D. Barlow, M. O'Callaghan, T. R. Glare, and T. A. Jackson. 1999. A model of insect-pathogen dynamics in which a pathogenic bacterium can also reproduce saprophytically. Proceedings of the Royal Society B 266:233–240.

Heesterbeek, J. A. P. 2002. A brief history of R_0 and a recipe for its calculation. Acta Biotheoretica 50:189–204.

Heesterbeek, J. A. P., and M. G. Roberts. 2007. The type-reproduction number T in models for infectious disease control. Mathematical Biosciences 206:3–10.

Hurford, A., D. Cownden, and T. Day. 2010. Next-generation tools for evolutionary invasion analyses. Journal of the Royal Society Interface 7:561–571.

Julian, T. R. 2016. Environmental transmission of diarrheal pathogens in low and middle income countries. Environmental Science: Processes and Impacts 18:944–955.

Kaitala, V., L. Ruokolainen, R. D. Holt, and J. K. Blackburn. 2017. Population dynamics, invasion, and biological control of environmentally growing opportunistic pathogen. Pages 213–245 *in* Modeling the transmission and prevention of infectious disease. Vol. 4. Advances in Environmental Microbiology. Springer, Cham.

Kinnula, H., J. Mappes, J. K. Valkonen, K. Pulkkinen, and L.-R. Sundberg. 2017. Higher resource level promotes virulence in an environmentally transmitted bacterial fish pathogen. Evolutionary Applications 10:462–470.

Kisdi, É. 2006. Trade-off geometries and the adaptive dynamics of two co-evolving species. Evolutionary Ecology Research 8:959–973.

———. 2015. Construction of multiple trade-offs to obtain arbitrary singularities of adaptive dynamics. Journal of Mathematical Biology 70:1093–1117.

Laanto, E., J. K. H. Bamford, J. Laakso, and L.-R. Sundberg. 2012. Phage-driven loss of virulence in a fish pathogenic bacterium. PLoS ONE 7:e53157.

Lanzas, C., K. Davies, S. Erwin, and D. Dawson. 2019. On modelling environmentally transmitted pathogens. Interface Focus 10:20190056.

Levin, B. R. 1996. The evolution and maintenance of virulence in microparasites. Emerging Infectious Diseases 2:93–102.

Lion, S., and J. A. J. Metz. 2018. Beyond R_0 maximisation: on pathogen evolution and environmental dimensions. Trends in Ecology and Evolution 33:458–473.

Martínez, J. L. 2014. Short-sighted evolution of bacterial opportunistic pathogens with an environmental origin. Frontiers in Microbiology 5:239.

Merikanto, I., J. T. Laakso, and V. Kaitala. 2018. Outside-host phage therapy as a biological control against environmental infectious diseases. Theoretical Biology and Medical Modelling 15:7.

Metz, J. A. J., S. A. H. Geritz, G. Meszéna, F. J. A. Jacobs, and J. S. van Heerwaarden. 1996. Adaptive dynamics: a geometrical study of the consequences of nearly faithful reproduction. Stochastic and Spatial Structures of Dynamical Systems 45:183–231.

Mikonranta, L., V. P. Friman, and J. Laakso. 2012. Life history trade-offs and relaxed selection can decrease bacterial virulence in environmental reservoirs. PLoS ONE 7:e43801.

Mikonranta, L., J. Mappes, J. Laakso, and T. Ketola. 2015. Within-host evolution decreases virulence in an opportunistic bacterial pathogen. BMC Evolutionary Biology 15:165.

Nas, M. Y., R. C. White, A. L. DuMont, A. E. Lopez, and N. P. Cianciotto. 2019. *Stenotrophomonas maltophilia* encodes a VirB/VirD4 type IV secretion system that modulates apoptosis in human cells and promotes competition against heterologous bacteria, including *Pseudomonas aeruginosa*. Infection and Immunity 87:10–12.

Peyraud, R., L. Cottret, L. Marmiesse, J. Gouzy, and S. Genin. 2016. A resource allocation trade-off between virulence and proliferation drives metabolic versatility in the plant pathogen *Ralstonia solanacearum*. PLoS Pathogens 12:e1005939.

Pilla, G., G. McVicker, and C. M. Tang. 2017. Genetic plasticity of the *Shigella* virulence plasmid is mediated by intra- and inter-molecular events between insertion sequences. PLoS Genetics 13:e1007014.

Platt, T. G., J. D. Bever, and C. Fuqua. 2012. A cooperative virulence plasmid imposes a high fitness cost under conditions that induce pathogenesis. Proceedings of the Royal Society B 279:1691–1699.

Pulkkinen, K., L.-R. Suomalainen, A. F. Read, D. Ebert, P. Rintamäki, and E. T. Valtonen. 2010. Intensive fish farming and the evolution of pathogen virulence: the case of columnaris disease in Finland. Proceedings of the Royal Society B 277:593–600.

Regoes, R. R., M. A. Nowak, and S. Bonhoeffer. 2000. Evolution of virulence in a heterogeneous host population. Evolution 54:64–71.

Roberts, M. G., and J. A. P. Heesterbeek. 2003. A new method for estimating the effort required to control an infectious disease. Proceedings of the Royal Society B 270:1359–1364.

Robino, E., A. C. Poirier, H. Amraoui, S. Le Bissonnais, A. Perret, C. Lopez-Joven, J. Auguet, et al. 2019. Resistance of the oyster pathogen *Vibrio tasmaniensis* LGP32 against grazing by *Vannella* sp. marine amoeba involves Vsm and CopA virulence factors. Environmental Microbiology 22:4183–4197.

Roche, B., J. M. Drake, and P. Rohani. 2011. The curse of the Pharaoh revisited: evolutionary bi-stability in environmentally transmitted pathogens. Ecology Letters 14:569–575.

Roff, D. A. 2000. Trade-offs between growth and reproduction: an analysis of the quantitative genetic evidence. Journal of Evolutionary Biology 13:434–445.

Sokurenko, E. V., R. Gomulkiewicz, and D. E. Dykhuizen. 2006. Source–sink dynamics of virulence evolution. Nature Reviews Microbiology 4:548–555.

Stearns, S. C. 1989. Trade-offs in life-history evolution. Functional Ecology 3:259–268.

Steinberg, K. M., and B. R. Levin. 2007. Grazing protozoa and the evolution of the *Escherichia coli* O157:H7 Shiga toxin-encoding prophage. Proceedings of the Royal Society B 274:1921–1929.

Sturm, A., M. Heinemann, M. Arnoldini, A. Benecke, M. Ackermann, M. Benz, J. Dormann, et al. 2011. The cost of virulence: retarded growth of *Salmonella typhimurium* cells expressing type III secretion system 1. PLoS Pathogens 7:e1002143.

Sumrall, E. T., Y. Shen, A. P. Keller, J. Rismondo, M. Pavlou, M. R. Eugster, S. Boulos, et al. 2019. Phage resistance at the cost of virulence: *Listeria monocytogenes* serovar 4b requires galactosylated teichoic acids for InlB-mediated invasion. PLoS Pathogens 15:e1008032.

Sundberg, L.-R., T. Ketola, E. Laanto, H. Kinnula, J. K. H. Bamford, R. Penttinen, and J. Mappes. 2016. Intensive aquaculture selects for increased virulence and interference competition in bacteria. Proceedings of the Royal Society B 283:20153069.

Sundberg, L.-R., H. M. T. Kunttu, and E. Valtonen. 2014. Starvation can diversify the population structure and virulence strategies of an environmentally transmitting fish pathogen. BMC Microbiology 14:67.

Tien, J. H., H. N. Poinar, D. N. Fisman, and D. J. D. Earn. 2011. Herald waves of cholera in nineteenth century London. Journal of the Royal Society Interface 8:756–760.

van Baalen, M., and M. W. Sabelis. 1995. The dynamics of multiple infection and the evolution of virulence. American Naturalist 146:881–910.

van den Driessche, P. 2017. Reproduction numbers of infectious disease models. Infectious Disease Modelling 2:288–303.

Walther, B. A., and P. W. Ewald. 2004. Pathogen survival in the external environment and the evolution of virulence. Biological Reviews 79:849–869.

White, C. V., B. J. Darby, R. J. Breeden, and M. A. Herman. 2016. A *Stenotrophomonas maltophilia* strain evades a major *Caenorhabditis elegans* defense pathway. Infection and Immunity 84:524–536.

References Cited Only in the Online Enhancements

Dieckmann, U., and R. Law. 1996. The dynamical theory of coevolution: a derivation from stochastic ecological processes. Journal of Mathematical Biology 34:579–612.